HiSST: 2nd International Conference on High-Speed Vehicle Science Technology
11–15 September 2022, Bruges, Belgium

Spectroscopic Characterization of Solid Rocket Motor Plume Radiation

Lars Steffens[1], Ali Gülhan[2]

Abstract

To gather information about both particle and gas phase temperatures inside a scaled solid rocket motor plume UV-VIS emission spectroscopy (UVVIS) and infrared emission spectroscopy (FTIR) have been used. Additionally, a position resolving two-color pyrometer technique in the visible spectrum range (Alumina Emission Measurements, AEM) has been developed to obtain a particle temperature distribution of the whole plume. These three methods have been applied during the ESA-EMAP project tests inside DLR's VMK facility of scaled solid rocket motor plumes [1]. This project pursued activities regarding the experimental modeling of alumina particulates in solid boosters (EMAP).

The UVVIS emission spectroscopy can be used to monitor the grey body radiation of the particle phase. This allows determining the particle phase temperature. FTIR spectroscopy allows the identification of gaseous species inside the plume such as CO_2, CO, HCL and H_2O. The emission lines of HCl can be used to determine the gas phase temperature of the plume. Both methods thus monitor the radiation intensity and the temperature over time at a certain position downstream the nozzle exit during the propellant combustion process. The AEM consists of two optical cameras which have been equipped with 10nm width optical bandpass filters to obtain intensity maps at two distinct wavelengths. The ratio of these intensity maps can be evaluated into a temperature distribution of the plume.

Keywords: *emission spectroscopy, solid rocket motor plume, particles*

Nomenclature

c – speed of light
h – Planck constant
k_B – Boltzmann constant
M_λ – spectral radiant exitance
T – temperature
T^* – apparent temperature
ϵ - emissivity
λ - wavelength

1. Introduction

For the characterization of solid rocket motor plumes, non-intrusive temperature measurements are an important part of understanding the thermochemical processes inside the plume, especially the particle phase of mainly aluminum oxide particles. The plume of solid rocket motor is a complex system, and not much matching data to validate especially simulations of particle phase exists. One goal of the ESA-EMAP project is to simultaneously measure many different parameters of both the particle and the gas phase of the plume. This publication describes the applied spectroscopic measurement techniques to gain information about the particle and the gas phase temperature and shows some exemplary results to demonstrate that they work in principle. A detailed summary and discussion of all ESA-EMAP results and their correlation to the other measurement technique results has to be a part of a future publication.

The non-intrusive measurement of particle temperatures in general relies on a thorough knowledge of the particle emissivity. The particle emissivity depends on the particle temperature, wavelength, on particle size, the phase state, and thickness of the oxide layer [2-4]. As the literature data on emissivity only usually covers only selected parameters and has incompatible or unknown parameters between different publications an accurate application highly relies on interpolation or extrapolation with high

[1] *German Aerospace Center (DLR e.V.), Linder Höhe, 51147 Köln, Germany, lars.steffens@dlr.de*

uncertainties. Thus, here only a first iteration step assuming wavelength independent emissivities is applied to gain an insight into the particle temperature data.

Gas phase temperatures where additionally measured by using IR emission lines of HCl, which can be clearly separated from the particle emission background. Emission spectroscopy is used for simplicity of the setup: broadband absorption spectroscopy in general gives more reliable results but is not feasible due to the high emission strength of the plume. Laser absorption spectroscopy is not feasible due to disturbance caused by the plume and the strong vibrations.

2. Experimental Setup

The experiments where performed within the scope of the ESA-EMAP project. For details and an overview about the project including project goals, experimental setup and diagnostic tools see [1]. In this publication only the feasibility of the three stated spectroscopic methods is evaluated.
The experiments were executed in the "Vertical test section Cologne" (VMK). VMK is a blow-down type wind tunnel featuring a vertical and free test section for tests in the subsonic to supersonic range starting from Mach 0.5 up to 3.2 [5-7]. The current experiments were conducted with a subsonic nozzle featuring an exit diameter of 340 mm.
A rocket motor was used for the execution of the experiments. This motor is shown in Fig. 1 and, as it can be seen, it is integrated via an upstream support (1) in the subsonic wind tunnel nozzle (2). For the main tests, end burner grains (7) are used to aim for constant conditions for all measurement techniques over one run test.

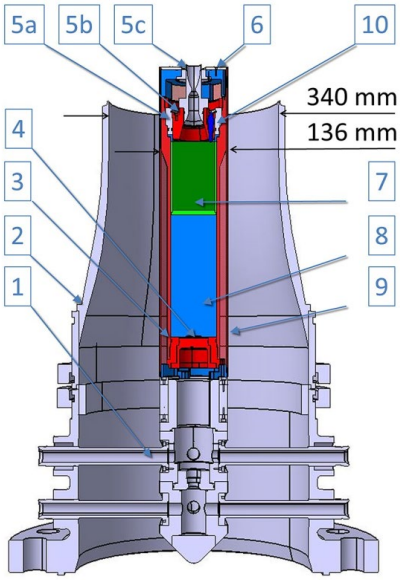

Fig 1. Sketch of the wind tunnel model with rocket motor (from [1]).

In frame of the project, three different solid propellants types were developed:
- HTPB1814 with 18% aluminum and 14% HTPB,
- HTPB0514 with 5% aluminum and 14% HTPB and
- HTPB0014Al2O3 with 14% HTPB and with 5% Al_2O_3 as inert filler.

where HTPB stands for hydroxyl-terminated polybutadiene.

UVVIS and FTIR are centered 30 mm axially above the nozzle exit. The setup of all three methods is given in section 3.

3. Experimental Methods

The plume of the scaled solid rocket motor emits light in the visible and infrared spectral range. This emitted light is a combination of the blackbody radiation of the hot liquid and solid particles inside the

plume on one hand as well as emission from exited atom and molecule species on the other hand. The emission spectra of atoms and molecules in the flow allow to identify the species and by comparison with numerical compute emission spectra to determine their temperature. The grey-body spectra emitted by particles allow estimating their temperature after a careful calibration of the spectrometer. Due to the different cooling behavior of the gas and particle phase of the plume, the temperature of both phases is expected to be different.

The UVVIS emission spectroscopy is used to gain information about the particle phase temperature locally with detailed spectral information. The AEM method is used to gain information about the particle phase temperature spatial distribution. FTIR emission spectroscopy is used to gain information about the gas phase temperature using the emission lines of HCl.

3.1. UVVIS Emission Spectroscopy

Light emitted by the plume in the spectral range of 200 nm to 850 nm is focused by a lens and coupled into fiber optics and by this transferred into an Ocean Optics USB2000 spectrometer (Fig 2.). Emission spectra are recorded over the complete duration of a test.

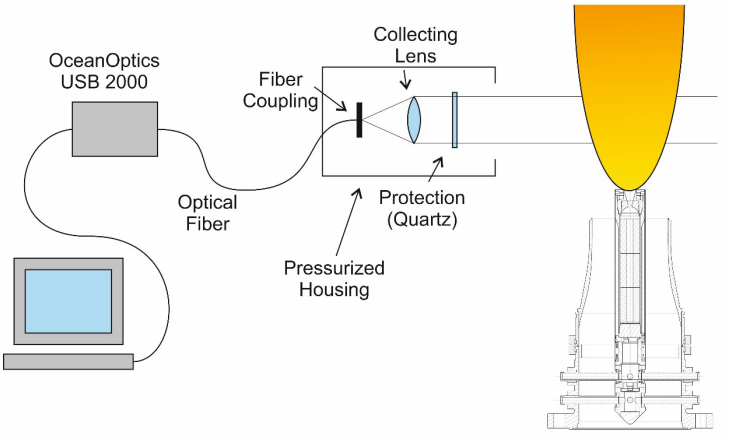

Fig 2. Sketch of the Experimental Setup of the UVVIS Emission Spectroscopy.

The optical setup and the spectrometer are placed in a pressurized box to protect them from the combustion products. The exposure time is manually adapted to the total intensity of the emitted light with a recording rate between 60 Hz and 80 Hz depending on the selected exposure time. A fiber coupling optic is adjusted to ensure the smallest possible diameter. By this a cylindric measurement volume of ~ 8 mm diameter is achieved, which is and is aligned axially above the nozzle exit at a distance of 30 mm to the exit.

A relative intensity calibration of the spectrometer in the VIS range is performed using a black body radiation source. For this calibration spectra have been recorded for temperatures of the black body source of 1100°C to 1500°C in steps of 50°C. The calibration is valid in the range from about 500 nm to about 800 nm. The lower end of the calibration range is caused by the low intensity of the black body radiation source below that wavelength. The upper end of the calibration range is caused by the low sensitivity of the spectrometer.

The spectral radiant exitance M_λ of a grey body surface with surface temperature T is given by [5]

$$M_\lambda = \epsilon(\lambda,T)\cdot\frac{c_1}{\lambda^5}\cdot\frac{1}{e^{\frac{c_2}{\lambda T}}-1} \approx \epsilon(\lambda,T)\cdot\frac{c_1}{\lambda^5}\cdot e^{-\frac{c_2}{\lambda T}} \quad (1)$$

with the radiation constants $c_1 = \frac{2\pi hc^2}{\lambda^5}$ and $c_2 = \frac{hc}{k_B}$. The approximation in (1) neglects the 1 in comparison to the exponential term, which is a valid assumption for the given wavelengths and

expected temperatures below 4000 K. Due to fact that the measured particle diameter size of the > 1 µm (1) the spectral dependency can be assumed to be valid.

A standard approach to get information about the particle temperature from a grey body spectrum is a two-color pyrometric approach: The quotient $\frac{M_{\lambda_2}}{M_{\lambda_1}}$ of the spectral radiant exitance at two distinct wavelengths λ_1 and λ_2 is calculated from a UVVIS spectrum, and by using the approximation in (1) one can calculate an apparent temperature T^* of

$$T^* \approx \frac{\frac{hc}{k_B}\left(\frac{1}{\lambda_1}-\frac{1}{\lambda_2}\right)}{ln\left(\frac{M_{\lambda_2}}{M_{\lambda_1}}\frac{\epsilon_{\lambda_1}}{\epsilon_{\lambda_2}}\frac{\lambda_2^5}{\lambda_1^5}\right)} \tag{2}$$

The temperature is denoted with an asterisk as T^* to clarify that the actual signal is a line-of-sight signal which is an integral of the single spectral radiant exitances over different temperatures and particle diameters, resulting in deviations from spectral dependency (1). Also, absorption of light passing obscuring particles and scattering of light either emitted from surrounding particles or from within the motor might change the actual spectral dependency.

The emissivity of aluminum oxide particles in both states has been studied and discussed in literature [2-4]. Besides temperature and wavelength, it depends on particle size, the phase state, and thickness of the oxide layer. The particle size was determined during the ESA-EMAP tests by a rocket plume collector (RPC) [9], an Aerodynamic Particle Sizer (APS) [1], and Direct image particle size determination (DIPSD) [1]. Phase state and oxide layer parameters are unknown. As the literature data on emissivity only usually covers only selected parameters and has incompatible or unknown parameters between different publications an accurate application highly relies on interpolation or extrapolation with high uncertainties. Thus, in the following only a first iteration step assuming wavelength independent emissivities is applied to gain an insight into the particle temperature data. So, when using $\frac{\epsilon_{\lambda_1}}{\epsilon_{\lambda_2}} = 1$ in (1) the resulting $T^*_{(0)}$ can be considered a zeroth order approximation.

A second approach to gain information about the particle temperature particularly developed for the ESA-EMAP project is using the logarithmic derivative of the spectral radiant exitance by the wavelength:

$$\frac{\frac{dM_\lambda}{d\lambda}}{M_\lambda} \approx \frac{\frac{d\epsilon}{d\lambda}}{\epsilon} - \frac{5}{\lambda} + \frac{\frac{hc}{\lambda^2 k_B T}}{e^{\frac{hc}{\lambda k_B T}}} \tag{3}$$

This can be resolved to an apparent temperature from the measured spectrum $M_\lambda(\lambda)$ when the logarithmic derivative of the particle emissivity function is known using the Lambert W function. When the (local) logarithmic derivative of the particle emissivity can be assumed to be negligible (or it is explicitly known), information about the particle temperature can be derived by a local analysis of a spectrum. The advantage of this method compared to the standard two-color approach is, that only one wavelength parameter is used and

Fig. 3 shows three UVVIS emission spectra of one test run at three different time stamps with. The propellants type of this test was HTPB0514. One can see the grey body radiation spectra of the particles. On this different atomic emission lines (mainly K and Na) and in the range from 485 nm to 510 nm and the emission lines of the L2F laser system used to measure particle velocities system can be seen. Fig. 4 shows the respective particle temperatures $T^*_{(0)}$ spectrum derived by logarithmic derivative at a given wavelength for each spectrum in Fig. 3 assuming a neglectable logarithmic derivative of the particle emissivity. The logarithmic derivative has been evaluated by a polynomial fit of second order over an interval of ±15 nm for the whole spectrum. The spectral ranges below 550 nm, between 580 nm and 650 nm, and between 740 nm and 800 nm are hidden due to the influences of the atomic and laser emission lines.

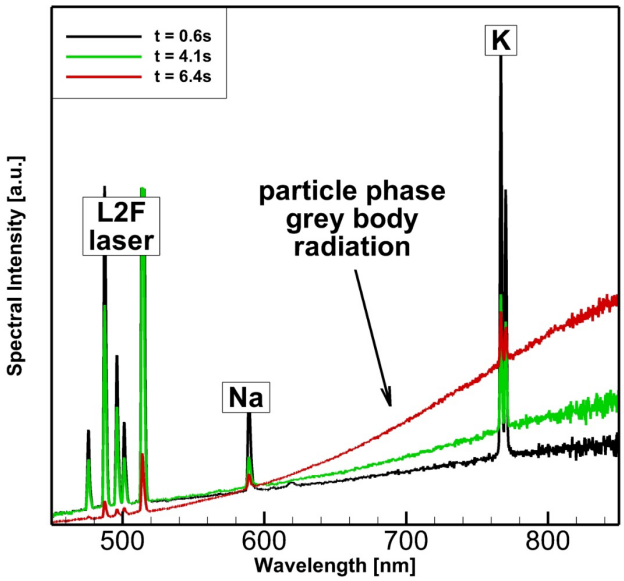

Fig 3. Example of three UVVIS spectra recorded during one test run.

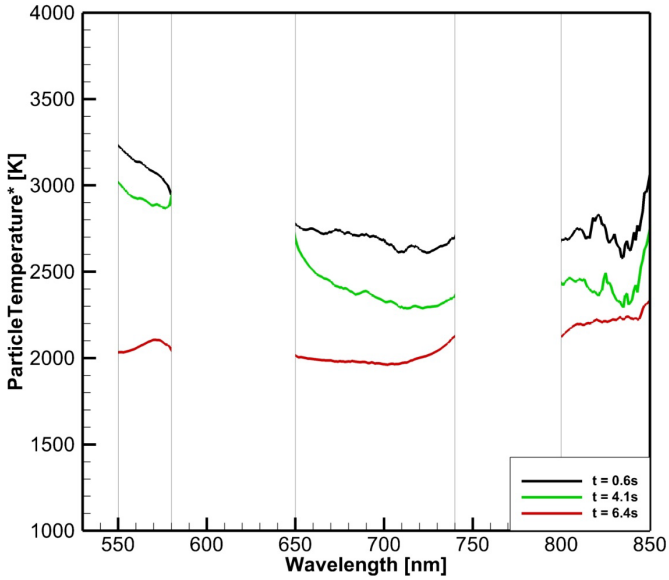

Fig 4. Example of three UVVIS spectra recorded during one test run.

The particle temperatures derived from 650°nm to 850 nm are mostly constant, suggesting that the assumption of a neglectable logarithmic derivative of ϵ is reasonable for a first approach. Fig. 5 depicts the particle temperatures over time for the wavelengths 570 nm (blue), 700 nm(green), and 820 nm (red). The temperatures derived at 700 nm and 820 nm are matching. The temperature derived at 570 nm is for most part of the test much higher than the other two. This might be an influence of the laser lines, or a hint on a non-neglectable logarithmic derivative of the particle emissivity at least in this spectral region. Figs. 6 shows particle temperatures over time determined by two-color pyrometry as described above, assuming a constant emissivity. The results vary by ±200 K depending on the exact spectral range analyzed. When using only the spectral range around 700 nm, the results are matching the results determined by logarithmic derivative.

The observed slight drop in the temperature occurs for most tests except those with propellant HTPB1814. The reason for the decrease might be a longer travel time due to the recessing propellant surface.

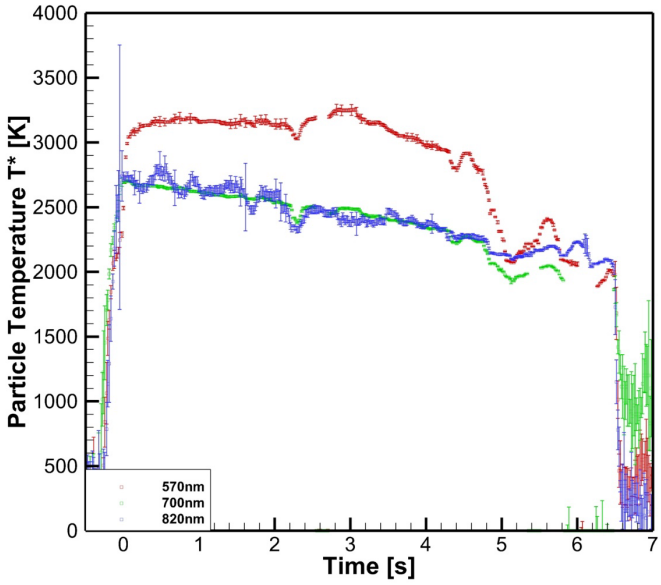

Fig 5. Particle Temperatures $T^*_{(0)}$ over time determined by logarithmic derivative method for three wavelengths.

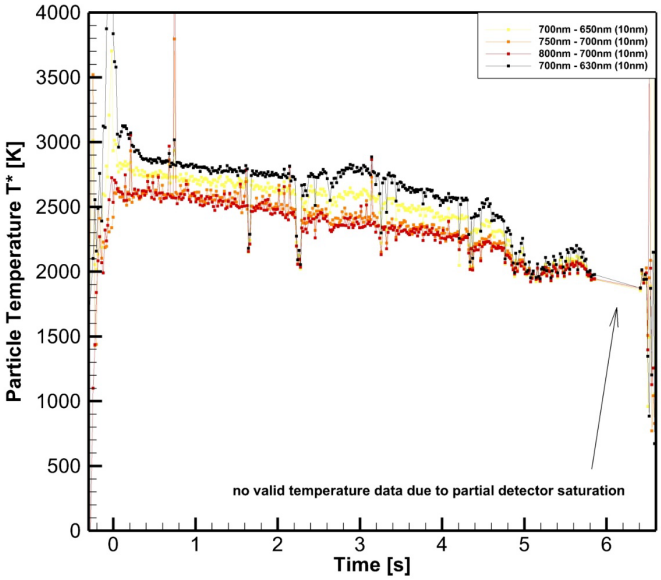

Fig 6. Particle Temperatures $T^*_{(0)}$ over time determined by two-color method for different wavelengths.

3.2. Alumina Emission Measurements (AEM)

The idea behind AEM is to record the emission of the alumina particles using a two-color setup consisting of two cameras operating at two different wavelengths allows eliminating the particle density dependence and allowing to determine position resolved information about the particle temperature distribution inside the plume. This setup corresponds to a position resolving two-color pyrometer (Fig. 7). This measurement technique is realized by two cameras in the visual range combined with two different narrow bandpass filter. The images are taken by using the two passes of a beam splitting mirror, to be able to exactly overlay the two images obtained at two different wavelengths. for a specific wavelength, at which no molecular or atomic emission lines are present, so that only particle emissions are observed. Examples of the raw images are shown in Fig. 8.

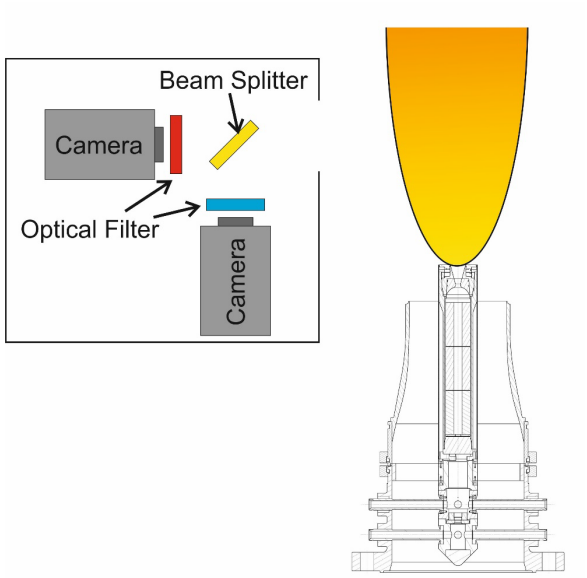

Fig 7. Sketch of the Experimental Setup of AEM.

Two monochromatic cameras with a 2048 x 2048 resolution were used. Band pass filters at 630 nm and 700 nm, each with a FWHM of 10 nm each have been placed directly in front of the objectives. As beam splitter a dichroic long pass mirror at a cut-on wavelength of 650 nm, a transmission band from 685 nm to 1600 nm, and a reflection band of 400 nm to 630 nm was used. In front of the dichroic mirror a protection glass was mounted to protect the optics from plume debris. The cameras were both focused onto a distance of 60 cm from the AEM container opening, which was the mounting distance of the container to the plume axis. A careful intensity calibration of the both cameras has been performed using a black body radiation source. For this calibration spectra have been recorded for temperatures of the black body radiation source of 1100°C to 1500°C in steps of 50°C. The optical view has been aligned to be perpendicular to the plume and centered to the main measurement position for all localized measurement techniques 30 mm above the nozzle exit. Both cameras were triggered with a common trigger signal at a trigger pulse separation of 34 ms (~29.4 Hz). The only parameter adapted for each test run was the exposure time to match the corresponding plume brightness. Longer exposure times capture less bright plumes, but also increase the motion blur of each frame.

This method relies on a knowledge of the quotient of the particle emissivities at the given wavelengths and in the given particle temperature range. As can be deduced from the results from Fig. 4 in the previous section, the results obtained by assuming the particle emissivities to be constant for two-color pyrometry at 630 nm and 700 nm are usually only up to 200 K larger than the ones determined by the more reliable method by logarithmic derivation. So, for the following evaluations and results an emissivity quotient of is assumed, and the radiation temperature can within these limits also be interpreted as particle temperature.

To obtain the temperature for each frame both camera images are background corrected. The background in most cases is only resulting from sensor noise. Afterwards both images are transformed to fit on top of each other. Then both images are intensity calibrated and equation (2) from the previous section is used to obtain the two-color particle temperature T^*.

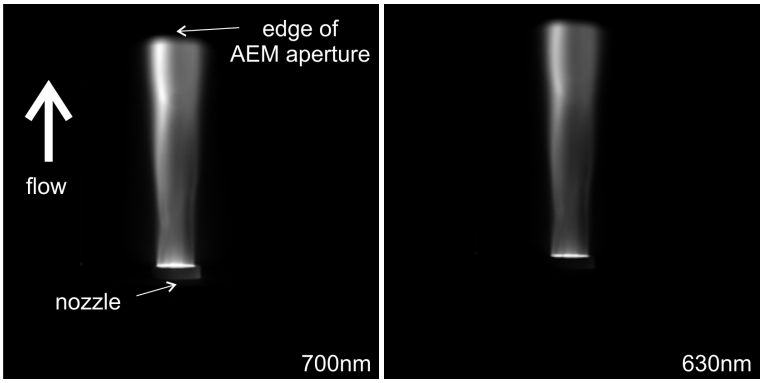

Fig 8. Sketch of the Experimental Setup of AEM.

Fig. 9 depicts the evaluated temperature data for one frame of a test with a HTPB1814 propellant. Pixels which are for at least one camera underexposed or overexposed are plotted white. Fig 10. compares the apparent particle temperatures $T^*_{(0)}$ determined by UVVIS (logarithmic derivative method at 700 nm) and AEM. The temperature value is the average taken of the data inside the 8 mm diameter circle 30 mm above the nozzle exit (as shown in Fig. 9) to be comparable to the UVVIS data. The error bars represent the corresponding standard deviation. The $T^*_{(0)}$values differ by the expected value of about 200 K.

For frames with low intensity, the temperatures are higher than expected, for some cases even much larger than expected. This effect can mostly likely be ascribed to an unwanted effect in the black level correction of the camera, which has been unnoticed for the calibration, and leads to a systematic error in the background level. The correction of this effect has to be part of future work. Table 3.400 shows a comparison of the AEM temperature data results compared to the UVVIS temperature data results. Whenever the camera illumination is high, the AEM temperatures are a good match to the UVVIS temperatures. In only three cases the temperature curves of UVVIS and AEM are uncorrelated.

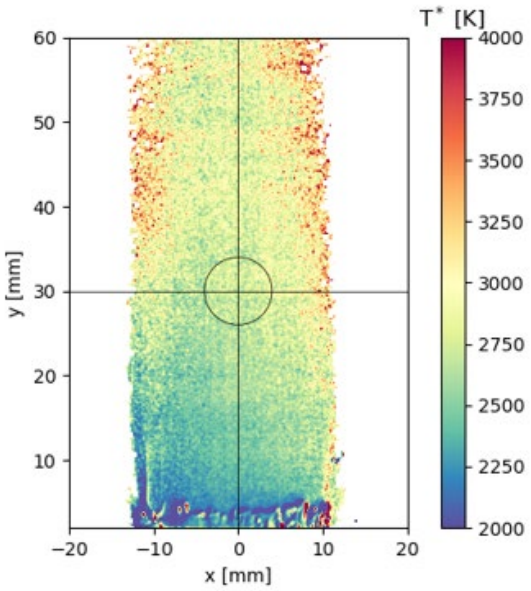

Fig 9. Example of the particle temperature distribution $T^*_{(0)}$ measured by AEM.

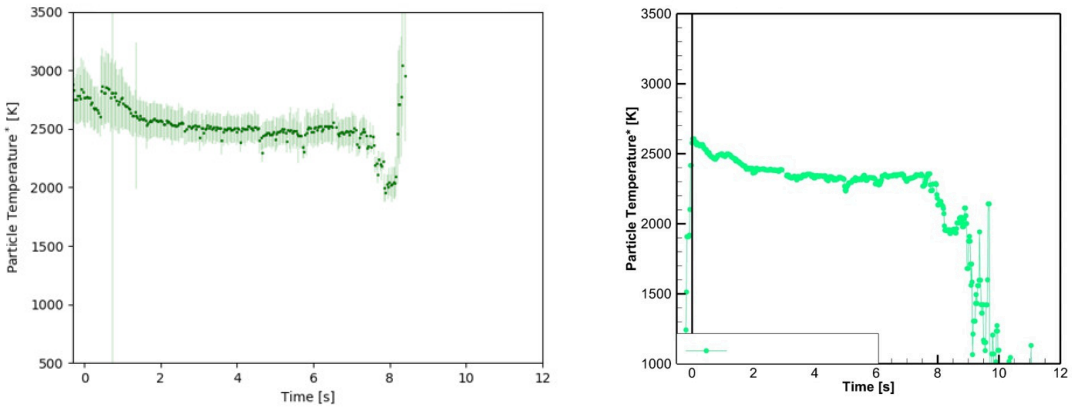

Fig 10. Comparison of $T^*_{(0)}$ over time measured by AEM (left, two-color method) and UVVIS (right, logarithmic derivative method).

3.3. FTIR Emission Spectroscopy

A Fourier-Transform Infrared (FTIR) Spectrometer using an MCT and an InSb detector is used for taking emission spectra in the infrared spectral range. It allows measure approximately 5 spectra per second in the spectral range from 2 µm to 8 µm with a spectral resolution of 1 cm^{-1}. To avoid saturation during the tests with 18 % aluminum content propellants, an additional Ge window has been installed inside the VMK to reduce the radiation amount incident to the spectrometer by about 50%.

These emission spectra can be used to determine molecular gas components of the plume, to analyze their relative radiation intensities, and to determine the gas temperature by comparing the emission lines of the molecular gas components to simulated emission spectra. In this case the emission lines of HCl are used to determine the gas temperature inside the plume. The spectrometer is positioned outside the VMK test chamber in front of a CaF_2 window. The position outside the main VMK chamber has been chosen to reduce the impact of VMKs vibrational noise during the test duration, and also to reduce the impact of corrosive gas components present in the plume. Due to the available window positions the spectrometer observes the plume under an angle of 13.5° with respect to the horizontal plane. Throughout this test campaign the lowest possible aperture diameter has been used, resulting in a cylindrical measurement volume of about 2.5 cm diameter. The center of the field of views is aligned to a height of 30 mm above the nozzle exit.

A spectrum of the measured infrared intensity over wavenumber for a test with propellant HTPB0514 is shown in Fig. 11. The spectrum consists on one hand of the signal of the grey body radiation of the particle phase of the plume, which can be seen as a continuous background in the complete depicted spectral range. Additionally, the molecular emission lines of several gas phase constituents can be seen: CO_2, CO, HCl, and H_2O. The ratio of particle grey body radiation intensity to molecular emission line intensity depends on the aluminum content of the propellant and is largest for 18 % aluminum content.

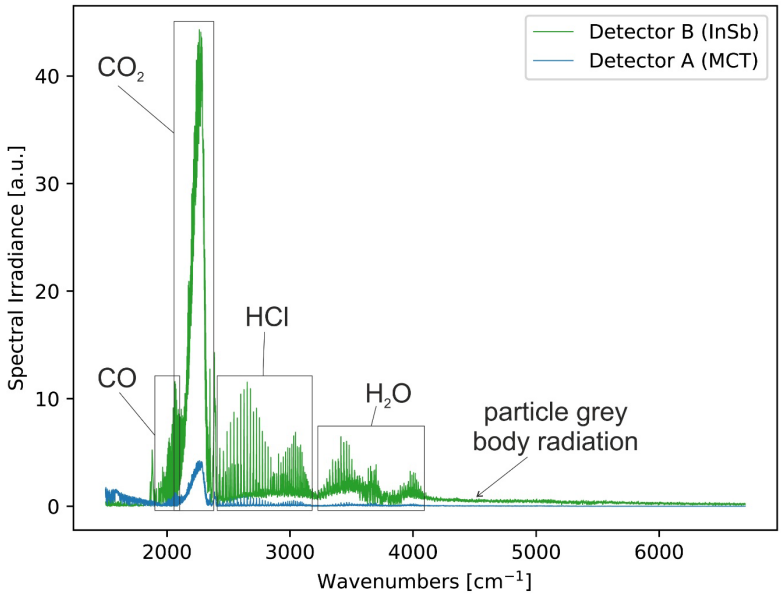

Fig 11. Example of an FTIR emission spectrum labelling the main emitting molecular species.

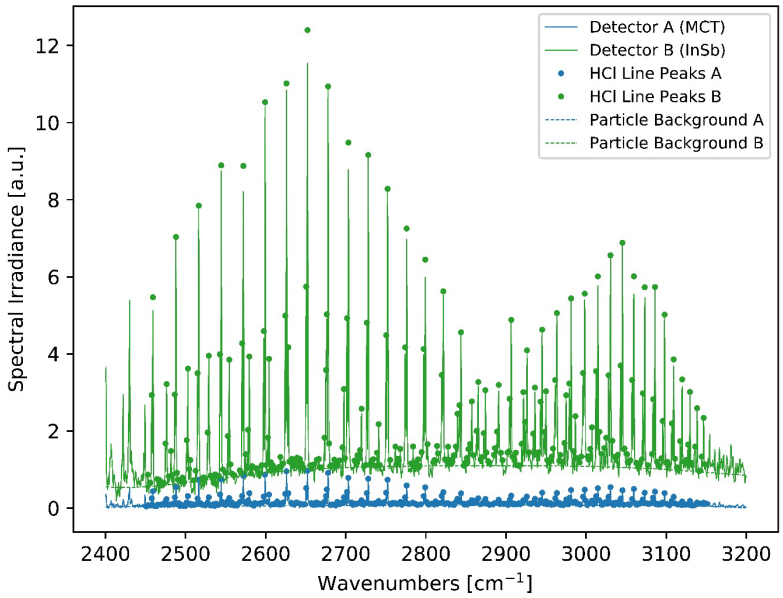

Fig 12. Magnification of Fig. 5 in the spectral region of HCl emission.

Fig. 12 shows a magnification of Fig. 11 in the spectral region of HCl emission. For this spectral region from 2450 cm^{-1} to 3150 cm^{-1}, the particle background has been determined as a polynomial regression. The polynomial background spectrum has been subtracted from the initial spectrum to get the molecular emission spectrum. For this molecular emission spectrum, a peak detection has been performed. As only parts of the spectra of one test run are mostly unaffected by vibrational noise, a manual selection of spectra suitable for temperature analysis has been carried out. The python based HAPI library has been used to simulate HCl emission spectra [10]. This library uses the data of the HITRAN database [11] to simulate emission spectra for homogeneous slabs of high temperature gases in chemical equilibrium up to temperatures of 3000 K. Parameters of this model are the gas temperature, the species partial pressure, the slab thickness, and a global scaling factor. The scaling factor is introduced to match the simulated to the measured spectra and has no physical meaning, as no absolute intensity calibration has been performed. The slab thickness is set to 1 cm for each evaluation, which is a good approximation for the order of magnitude of the thickness of the plume.

The slab thickness has only a linear effect on the resulting spectra in the expected regime of temperatures and pressures with negligible impact on the shape of the spectrum. Its effect can thus not be distinguished from the effect of the scaling factor, which allows for much less costly calculations when varied. So, the slab thickness is kept fixed. Peak detection is then also applied on the simulated spectra to allow for a simple comparison of experimental and simulated spectra. To compare simulated to experimental spectra an objective function is calculated as follows. Only peaks with a magnitude over a certain threshold are selected from the experimental spectrum, to omit low peaks falsely detected or distorted by noise. Those peaks are mapped by wavenumber to the peaks of the simulated spectrum. The objective function is the sum of both the quadratic distances between the measured and the corresponding simulated peaks, as well as the quadratic magnitude of simulated peaks, which don't have a corresponding experimental peak above the mentioned threshold. Peaks of the simulated spectrum with a low magnitude are ignored also for the calculation of the objective function.

To find the spectrum parameters that result in a minimum of the objective function with comparatively low computational power, a multivariate minimizer is applied. Fig. 13 shows the optimization results for both detectors, comparing the peaks of the HAPI model with the measured emission lines in the spectral range from 2500 cm^{-1} to 2900 cm^{-1}. and the resulting simulated spectra are similar to the experimental ones. The temperatures are in the range of 1850 K, which is in the expected range as calculated with the RPA software [12] for the gas phase temperature at the nozzle exit. The optimization does not provide a consistent pressure, as the influence of the pressure to the line strength is negligible.

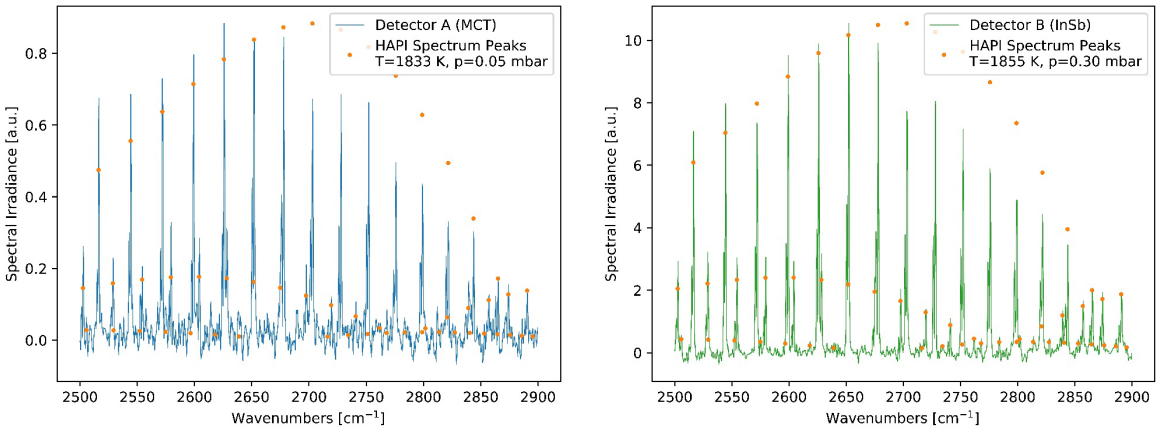

Fig 13. Optimization results for both detectors, comparing the peaks of the HAPI model with the measured emission lines.

The difference of the measured and simulated line peaks is usually small at the beginning of a test and increases with the progress of the test run. The difference between modelled and observed spectra might be caused by several effects: the expected inhomogeneous local gas temperature inside the measurement volume is not considered in the current HAPI model implementation, leading to possible deviations Another reason for the deviations may be mechanical vibrations in the VMK. They can influence the FTIR measurements, as a main component of the spectrometer is a moving mirror. This can be noticed in the latter part of each test run, when the spectra get noisy. To study the actual impact of all these effect on the results has to be the outcome of future work.

4. Discussion and Outlook

UVVIS emission spectra and AEM allow to get a first iteration step on the particle phase temperature assuming constant particle emissivity. The data obtained by both methods is comparable for most test cases. Further investigation of the spectral distribution (UVVIS) may lead to possible corrections of the constant emissivity assumptions and thus to more accurate temperature values.

The FTIR emission spectra can be evaluated to determine the gas phase temperature with results in the expected range. Slight differences between modelled and observed spectra occur, whose origin is still to be investigated and implemented into an improved model for the simulation.

References

1. Saile, D., Allofs, D., Kühl, V. et al.: Characterization of SRM plumes with alumina particulate in subscale testing. CEAS Space J 13, 247–268 (2021)
2. Sarou-Kanian, V., Rifflet, J. C. & Millot, F., IR Radiative Properties of Solid and Liquid Alumina: Effects of Temperature and Gaseous Environment. International Journal of Thermophysics, 26, pp. 1263-1275 (2005)
3. Anfimov, N. et al., Analysis of mechanisms and the nature of radiation from aluminum oxide in different phase states in solid rocket exhaust plumes. s.l., American Institute of Aeronautics and Astronautics (AIAA) (1993).
4. Lynch, P., Krier, H. & Glumac, N. Emissivity of Aluminum-Oxide Particle Clouds: Application to Pyrometry of Explosive Fireballs. Journal of Thermophysics and Heat Transfer, 24, pp. 301-308 (2010)
5. Triesch, K., Krohn, EO.: Die Vertikale Meßstrecke der DFVLR in Köln-Porz (Stand 1986), DFVLR-Mitt. 86-22. Wissenschaftliches Berichtswesen der DFVLR, ISSN 0176-7739, Postfach 906058, 5000 Köln 90 (1986)
6. DLR ACG Vertical Test Section Cologne (VMK), Supersonicand Hypersonic Technology Department. http://www.dlr.de/ as/en/desktopdefault.aspx/tabid-194/407_read-5445/ (2019). Accessed 14 Mar 2019
7. Saile, D., Kirchheck, D., Gülhan, A., Banuti, D.: Design of a hot plume interaction facility at DLR Cologne. In: Proceedings of the 8th European symposium on aerothermodynamics for space vehicles, Lisbon, Portugal, (2015)
8. Planck, M., The Theory of Heat Radiation. P. Blakiston's Son & Co. (1914)
9. Maggi, F., Carlotti, S., et al.: Determining the particles size in solid rocket motor plume. In: International conference on flight vehicles, aerothermodynamics and re-entry missions and engineering (FAR) (2019)
10. Kochanov, R., R. Gordon, L. Rothman, P. Wcislo, C. Hill, and J. Wilzewski, HITRAN Application Programming Interface (HAPI): A comprehensive approach to working with spectroscopic data, Journal of Quantitative Spectroscopy and Radiative Transfer, vol. 177, pp. 15-30, (2016)
11. Gordon, I., L. Rothman, and C. e. a. Hill, The HITRAN2016 Molecular Spectroscopic Database, Journal of Quantitative Spectroscopy and Radiative Transfer, Journal of Quantitative Spectroscopy and Radiative Transfer, vol. 203, pp. 3-69, (2017)
12. Ponomarenko, A., RPA-tool for rocket propulsion analysis, Space propulsion conference (2014)